

High-order cyclo-Raman scattering of a laser by a single electron

Y. J. Ding and A. E. Kaplan

Department of Electrical and Computer Engineering, The Johns Hopkins University, Baltimore, Maryland 21218

(Received 20 August 1987; revised manuscript received 22 February 1988)

“Cyclo-Raman resonance” of a single electron (i.e., cyclotron motion of an electron driven by optical fields) in the n th order at the cyclotron frequency Ω_c can be excited by biharmonic laser beams with their frequencies ω_1 and ω_2 such that $\omega_1 - \omega_2 \approx n\Omega_c$. This effect exhibits hysteresis, “prohibited” and “allowed” orbits of excitation, phase multistability, and the optical Stark effect.

The interaction of radiation with a slightly relativistic single electron can result in strong nonlinear effects¹⁻⁶ constituting the most fundamental mechanism of nonlinear interaction of light with matter.³ These effects include hysteresis and bistability in cyclotron resonance of a free electron predicted in Ref. 1 and experimentally observed in Ref. 2, high-order optical subharmonics excitation,⁵ and multiphoton optical resonances.^{4,6} The latter processes consist of the excitation of a free electron (at the cyclotron frequency Ω_c) driven by a biharmonic laser with frequencies ω_1 and ω_2 such that $\omega_1 - \omega_2 \approx \Omega_c$ (three-photon resonance^{4,6}) or $\omega_1 - \omega_2 \approx 2\Omega_c$ (four-photon resonance⁴). Under biharmonic pumping, in the first approximation for each optical photon with higher frequency ω_1 , one optical photon with lower frequency ω_2 , as well as one or two photons with the cyclotron frequency Ω_c , are emitted. It is natural, therefore, to regard these processes as “stimulated cyclo-Raman scattering” of the first and the second orders, respectively.

In this paper, we show that with a low driving laser power it is feasible to observe cyclo-Raman excitation and scattering of an arbitrary n th order, with the difference between driving laser frequencies being $\omega_1 - \omega_2 \approx n\Omega_c$ when n is an integer. For any order n , the cyclo-Raman resonances exhibit “prohibited” and “allowed” cyclotron orbits (which results in multiple isolated branches of solutions,⁶ the so-called isolas), n possible equidistant phase states (which results in phase multistability for $n > 1$), the optical Stark shift (i.e., an intensity-dependent shift of the eigenfrequency), and multiwave mixing effects.

Consider a single electron in a homogeneous magnetic field $\mathbf{H}_0 = \mathbf{h}H_0$ which gives rise to a cyclotron resonance with the initial (i.e., unperturbed) frequency $\Omega_c = eH_0/m_0c$. The electron is illuminated by optical waves with their frequencies being ω_1 and ω_2 , respectively (with $\omega_1 > \omega_2$). We designate $\omega_1 - \omega_2 = n\Omega_c$ and assume that neither ratio $(\omega_1 + \omega_2)/\Omega_c$ nor $\omega_{1,2}/\Omega_c$ is an integer (this excludes higher-order subharmonics⁵ and can readily be arranged by the proper frequency tuning). We choose the propagation configuration such that all the traveling waves \mathbf{E}_j propagate in the plane normal to \mathbf{H}_0 with their polarizations parallel to \mathbf{H}_0 (see inset in Fig. 1). We describe the motion of the electron by its momentum \mathbf{p} and radius vector \mathbf{r} , and introduce the dimensionless

quantities $\rho = \mathbf{p}/m_0c$, $\mathbf{f}_j = \mathbf{E}_j/H_0 = e\mathbf{E}_j/m_0c\Omega_c$, and $\mathbf{q}_j = \mathbf{k}_j/k_j$, where $k_j = \omega_j/c$.

Following Refs. 1-6, we treat the problem classically, which is justified by a relatively high (and therefore classical) energy of electron excitation. Indeed, even in the case of lowest-order cyclo-Raman scattering, we typically obtain $\rho_c \approx \beta_c \approx 10^{-3}$, which corresponds to the energy of ≈ 0.25 eV, i.e., to the excitation of a few hundreds of Landau levels. Using a conventional Lorentz equation (modified to include damping due to synchrotron radiation^{4,7}) and following procedure,⁴ we expand the momentum ρ as $\rho = \rho_c + \rho_{nc}^{(1)} + \dots$, where ρ_c (normal to \mathbf{h}) is a cyclotron component corresponding to a pure revolution

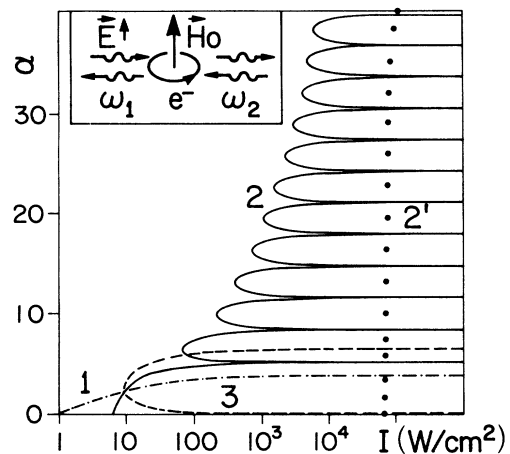


FIG. 1. Maximal and minimal values of excitation parameter α proportional to the total electron momentum p_c [see the text between Eqs. (6) and (7)] vs the intensity of driving waves I . Curve 1 (dot-dashed line) and the lower branch of curves 2 (solid lines) correspond to the maximum of the main hysteresis for the cyclo-Raman scattering with $n = 1$ (Ref. 6) and $n = 2$, respectively, the next one above the lower branch of curves 2 to the first isola, etc. Curve 3 (dashed line) corresponds to the maximal and minimal excitation of the first isola for $n = 3$. Areas surrounded by each curve correspond to allowed excitation; areas between them, to prohibited excitation. The inset depicts the propagation configuration. Curve 2' (dotted line) corresponds to the maximal excitation for a different configuration of the cyclo-Raman scattering with $n = 2$ (Ref. 4).

of the electron around some fixed center ($\mathbf{r}=0$) with the frequency $\Omega \approx \Omega_c / \gamma_c$, and the noncyclotron components of various orders ρ_{nc} include oscillations with all the other, nonresonant, frequencies. The cyclotron motion is governed then by the equation⁴

$$\Omega_c^{-1} \dot{\rho}_c - \gamma_c^{-1} (\rho_c \times \mathbf{h}) + \Gamma \gamma_c \rho_c = \mathbf{F}_c^{(1)} + \mathbf{F}_c^{(2)} + \dots, \quad (1)$$

where $\mathbf{F}_c^{(s)}$ are cyclotron components of various sth-order forces $\mathbf{F}^{(s)}$, $\Gamma = 2e^2 \Omega_c / 3m_0 c^3 \lll 1$ is a synchrotron damping parameter, and $\gamma_c = (1 + \rho_c^2)^{1/2}$. In the case of optical driving⁴ $\mathbf{F}_c^{(1)} = 0$, and the first meaningful term contributing to this excitation is cyclotron component $\mathbf{F}_c^{(2)}$ of the force

$$\mathbf{F}^{(2)} = \gamma_c^{-1} \sum_j \mathbf{q}_j (\mathbf{f}_j \cdot \rho_{nc}^{(1)}) - \frac{\rho_c \times \mathbf{h}}{2\gamma_c^3} (\rho_{nc}^{(1)})^2. \quad (2)$$

Here $\mathbf{f}_j \equiv \mathbf{f}_j(\omega_j t - \mathbf{k}_j \cdot \mathbf{r})$ are all the traveling waves participating in the interaction, and $\rho_{nc}^{(1)}$ for the chosen configuration was found to be⁶

$$\rho_{nc}^{(1)} = \sum_j (\Omega_c / \omega_j) \mathbf{f}_j(\omega_j t - \mathbf{k}_j \cdot \mathbf{r}_c - \pi/2), \quad (3)$$

where $\mathbf{r}_c = c \gamma_c^{-1} \int \rho_c dt = -c(\Omega \gamma_c)^{-1} (\rho_c \times \mathbf{h})$. In contrast to the hysteretic resonance at the main frequency,¹⁻³ cyclo-Raman excitations are attributed to the so-called nonlinear radiation Lorentz and “fast” relativistic mechanisms;⁴ see the first and second terms on the right-hand side of Eq. (2), respectively. The former mechanism here is originated by *magnetic* fields of optical waves, whereas the latter one is due to modulation of relativistic electron mass $m(t) = m_0 \gamma(t)$ caused by fast but slight noncyclotron (optical) perturbations of a microwave cyclotron electron motion. Once the cyclotron motion is excited, though, it is only the “slow” relativistic mass effect [see below, Eq. (5)] that acts to limit the excitation energy and to form hystereses or isolas.

We further assume that $\mathbf{h} = \hat{\mathbf{e}}_z$ and the driving radiation at both frequencies ω_1 and ω_2 forms standing-wave patterns with all the waves propagating along the same axis x , i.e., $\mathbf{q}_{j\pm} = \mp \hat{\mathbf{e}}_x$; see inset in Fig. 1. For each frequency ω_j ($j=1,2$) there are two counterpropagating traveling waves $\mathbf{f}_{j\pm} = (f_j/2) \hat{\mathbf{e}}_z \sin(\omega_j t \pm k_j x + \psi_{j\pm})$ with the same amplitude $f_j/2$; their phases $\psi_{j\pm}$, in general, could be different. The equilibrium cyclotron motion is achieved when the center of the cyclotron orbit coincides with a node of one of the standing waves and simultaneously with an antinode of the other one if n is odd, and with nodes of both standing waves (or their antinodes) if n is even. Therefore one of the choices for the phases in the equation for $\mathbf{f}_{j\pm}$ is $\psi_{1+} = n\pi$, $\psi_{1-} = 0$, and $\psi_{2\pm} = 0$. At this point, the average radiation forces of all the waves acting upon the electron cancel each other out and therefore the trapping potential (although weak) can be excluded from consideration (which is why the standing-wave configuration is chosen for this calculation).

Substituting $\rho_{nc}^{(1)}$ in the form of Eq. (3) into Eq. (2), assuming ρ_c in the form

$$\rho_c = \rho_c [\sin(\Omega t + \phi) \hat{\mathbf{e}}_x + \cos(\Omega t + \phi) \hat{\mathbf{e}}_y],$$

where ρ_c and ϕ are the slowly varying cyclotron momentum amplitude and phase, respectively, separating the cyclotron component $\mathbf{F}_c^{(2)}$ out of $\mathbf{F}^{(2)}$ and substituting it into Eq. (1), we obtain two scalar equations for the dynamics of ρ_c and ϕ ,

$$\Omega_c^{-1} \gamma_c \dot{\rho}_c = -\Gamma \gamma_c^2 \rho_c + \mu Q_+ \sin \theta_n, \quad (4)$$

$$\Omega_c^{-1} \gamma_c \rho_c \dot{\phi} = -(\gamma_c \Omega / \Omega_c - 1 - S) \rho_c + \mu (Q_- - \beta_c^2 Q_+ / n) \cos \theta_n, \quad (5)$$

where $\theta_n = n(\phi - \pi/2)$, and Q_{\pm} are defined as

$$Q_{\pm} = J_{n-1}(\alpha) \pm J_{n+1}(\alpha) + \frac{n\Omega}{\omega_1 + \omega_2} [J_{n-1}(n\beta_c) \pm J_{n+1}(n\beta_c)]. \quad (6)$$

In Eqs. (4)–(6) $J_\nu(z)$ is the ν th-order Bessel function of first kind, $\alpha_{1,2} \equiv \omega_{1,2} \rho_c / \Omega_c$, $\alpha \equiv \alpha_1 + \alpha_2$, $\beta_c = v/c = \rho_c / \gamma_c$, the term S is defined as

$$S = \frac{1}{8} \sum_{i=1}^2 f_i^2 \left\{ \frac{\Omega^2}{\omega_i^2} + (-1)^{ni} \left[\left(\frac{\Omega^2}{\omega_i^2} + 2 \right) J_0(2\alpha_i) + 2J_2(2\alpha_i) \right] \right\}, \quad (7)$$

and μ is a driving parameter defined as

$$\mu = f_1 f_2 (\Omega_c / \omega_1 + \Omega_c / \omega_2) / 8.$$

The term S in Eq. (7) was identified in Ref. 6 as the optical (i.e., intensity-dependent) Stark shift of the eigenfrequency Ω [also see Eq. (8) below]. The term γ_c inside the first set of parentheses on the right-hand side (rhs) of Eq. (5) reflects the “slow” relativistic change of electron mass which gives rise to hysteresis or isola regimes. It should be noted that the signs in front of terms with $(-1)^{ni}$ in Eq. (7) must be changed if the location of the center of orbit with respect to both of the standing waves is chosen in such a way that $\psi_{1-} = 0$, $\psi_{1+} = (n-1)\pi$, $\psi_{2-} = 0$, and $\psi_{2+} = \pi$. The steady-state regime follows from Eqs. (4) and (5) if $d/dt = 0$, in particular,

$$\gamma_c \Omega / \Omega_c - 1 = S \pm \rho_c^{-1} [Q_-(\alpha) - \beta_c^2 Q_+(\alpha) / n] \times (\mu^2 - \rho_c^2 \Gamma^2 \gamma_c^4 / Q_+^2)^{1/2}, \quad (8)$$

Our stability analysis of Eqs. (4) and (5) showed that the upper sign in Eq. (8) corresponds to stable states, and the lower to unstable ones; see Fig. 2.

The phase stability is an important issue critical for maintaining a coherent excitation of a single electron, since a single electron is a very high-finesse system. For example, in the case of $\lambda_c = 2$ mm, $\Gamma \approx 0.6 \times 10^{-11}$, which corresponds to the half-linewidth of 0.9 Hz. The estimate in Refs. 4 and 6 shows that the critical laser intensity to obtain a hysteretic first-order cyclo-Raman effect is approximately 48 mW/cm², which allows one to use a He-Ne laser even with sub-mW total power. In this case the effective driving frequency Ω is formed by the difference between two laser modes $\Omega = \omega_1 - \omega_2$. Currently available stabilized He-Ne lasers can produce a frequency sta-

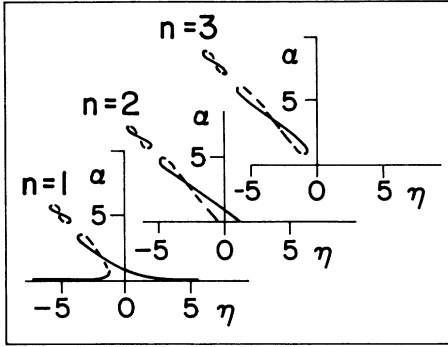


FIG. 2. Excitation parameter α vs frequency detuning parameter η (as defined in the text) for the cyclo-Raman excitation of different orders ($n=1,2,3$), with the fixed driving amplitude. The solid branches in the curves correspond to stable states, the broken ones to unstable states.

bility better than 0.1 Hz.⁸ Therefore this stability is sufficient for observation for the proposed effect, even if one assumes that the frequency fluctuations at both modes (ω_1 and ω_2) are completely independent. Furthermore, the dominant source of laser frequency fluctuations is a laser resonator,^{8,9} which suggests strong phase coherence *between* neighboring laser modes radiated by the same laser. In such a case, assuming $\Delta\Omega$ and $\Delta\omega$ to be frequency fluctuations of the effective driving frequency Ω and laser frequency, respectively, one finds that $\Delta\Omega \approx \Delta\omega(\Omega/\omega)$, where $\omega = (\omega_1 + \omega_2)/2$, which suggests that the fluctuations at the frequency Ω may be reduced by a factor $\sim \omega/\Omega$. In a typical case this reduction can be as large as $\sim 10^3$, which may result in a linewidth $\Delta\Omega$ significantly smaller than that of a synchrotron radiation linewidth. This illustrates potential advantages of cyclo-Raman laser excitation over conventional methods of cyclotron excitation exploiting rf or microwave sources.

It is readily seen from Eqs. (4) and (5) that there are n equally possible different equidistant states of the phase $\phi_{u,l}^m$ ($m=0,1,\dots,n-1$) for both stable and unstable branches by $\phi_{u,l}^m = \phi_{u,l}^0 + 2\pi m/n$. Which one of n stable phase states is excited depends on the initial condition of excitation. Therefore *phase multistability* (i.e., multiple stable phase states analogous to that in n -stable parametric frequency dividers¹⁰) is expected.⁴

Isolated branches of steady-state excitation (the so-called isolas similar to isolas in other areas of nonlinear physics¹¹) appear when driving force μ , and therefore kinetic energy, of the electron increases. These isolas occur because of a spatially oscillating wave pattern of driving radiation in the plane of cyclotron motion attributed to the particular propagation configuration used here. This is confirmed by comparison with Ref. 4, in which four-photon resonance (i.e., essentially, the cyclo-Raman scattering with $n=2$) was considered with two waves propagating *parallel* to \mathbf{H}_0 . It was shown in Ref. 4 that this propagation configuration, which does *not* form a spatially oscillating wave pattern in the plane of cyclotron motion, does not give rise to isolas either. The isolas in consideration can be obtained even in the case of low-

energy excitation, $\rho_c^2 \ll 1$ (but sufficiently high parameter α). In such a case, the expression in the square root in Eq. (8) can be rewritten as

$$\mu^2 - \Gamma^2 \rho_c^2 \alpha^2 / 4n^2 J_n^2(\alpha);$$

therefore the steady-state excitation is allowed only if

$$2n\mu |J_n(\alpha)| \geq \alpha \rho_c \Gamma. \quad (9)$$

This condition determines the maximal possible momentum $(\rho_c)_{\max}$ for any given driving amplitude μ . Equation (9) shows, on the other hand, that when μ exceeds some level, there are ranges of momentum ρ_c [such that $\rho_c < (\rho_c)_{\max}$] in which the steady-state excitation *does not exist*, i.e., some orbits are “prohibited” (note that $r_c = \rho_c/k_c \approx \beta_c/k_c$, where $k_c = \Omega_c/c$). For sufficiently large α , Eq. (9) predicts the radii of prohibited orbit, $r_{\text{proh}} \approx (2l+1)\bar{\lambda}/8$, where l is an integer and $\bar{\lambda} = 4\pi c/(\omega_1 + \omega_2)$. Prohibited orbits correspond to the destructive interaction of both of the waves with respect to the electron, as opposed to the constructive interaction pertinent to “allowed” orbits forming isolas. As the intensity of driving waves (or μ) increases, the first isola is formed, then the second, and so on.

The critical driving parameter μ required to observe the m th isola of n th order cyclo-Raman excitation is determined by Eq. (9) (with the equality sign), in which instead of α one has to substitute the m th positive root of the equation $(n-2)J_{n-1}(\alpha) - (n+2)J_{n+1}(\alpha) = 0$. In the case $n=1$, the first isola appears⁶ at $\alpha \approx 5$ with the critical laser intensity as low as ≈ 77 W/cm² ($\lambda_c \approx 2$ mm, $f_1 = f_2$). In the cyclo-Raman scattering with $n=2$, a cyclotron oscillation cannot be excited at all (see Fig. 2) unless driving amplitude exceeds the threshold $\mu_0 \approx 2\Gamma\Omega_c/(\omega_1 + \omega_2)$, which corresponds to the laser intensity ≈ 6.6 W/cm²; see the lower branch of curves 2 in Fig. 1. Such intensity can again be obtained using a focused cw He-Ne laser. As the laser intensity increases, in addition to the hysteretic resonance,⁴ one can observe the formation of isolas. For the propagation configuration considered here, the critical laser intensity for a cyclotron excitation is about three to five orders of magnitude lower, compared with that for the configuration.⁴ However, once the cyclotron oscillation is excited, the maximal kinetic energy of the electron in the configuration⁴ dramatically increases as the driving laser intensity I increases, the maximal kinetic energy of the electron being $\gamma_{\max} - 1 = (I/I_0)^{1/4} - 1$, where $I_0 = 0.66 \times 10^5$ W/cm² (see curve 2' in Fig. 1), whereas the energy of the first isola in the configuration considered here reaches saturation at a relatively low level.

Equations (8) and (9) show that for all $n \geq 3$, the cyclo-Raman scattering with arbitrary low ρ_c^2 cannot be excited, i.e., there is some minimal level of possible kinetic energy of electron excitation; this corresponds to the so-called hard excitation. Therefore, for the cyclo-Raman scattering with $n \geq 3$, only isolas excitation is possible, although the critical laser intensity remains relatively low (e.g., the intensity ~ 9.7 W/cm² is required to observe the first isola for $n=3$). In Fig. 2, the excitation parameter α is depicted versus the frequency detuning parameter

$$\eta = \text{sgn}(\Delta) \sqrt{2|\Delta|} (\omega_1 + \omega_2) / \Omega_c$$

($\Delta = \Omega / \Omega_c - 1$, and “sgn” is the sign function) at the driving amplitude $\mu = 50\Gamma\Omega_c / (\omega_1 + \omega_2)$ for cyclo-Raman excitation of the various orders n . The “self-crossing”⁶ of steady-state characteristics seen in Fig. 2 is unlikely to be observed in the experiment since one of the two self-crossing branches in an isola is unstable.

The total power P_c of the synchrotron radiation at the cyclotron frequency Ω in the low-relativistic case ($\rho_c^2 \ll 1$) can be written as⁷ $P_c \approx \Gamma\rho_c^2\Omega_c m_0 c^2$. The noncyclotron momentum $\rho_{nc}^{(1)}$ (parallel to \mathbf{H}_0) oscillates at combination frequencies $\omega_{1,2} \pm l\Omega$, Eq. (3), where l is an integer, and therefore gives rise to the stimulated dipole radiation at these frequencies (with a polarization parallel to \mathbf{H}_0), which can also be regarded as multiwave mixing. It can be shown that at low excitation the power P_1 absorbed from the higher laser frequency ω_1 and the power P_2 radiated at the lower frequency ω_2 obey the Manley-Rowe relationships $P_1 = -P_c\omega_1/n\Omega$ and $P_2 = P_c\omega_c/n\Omega$. This reflects a quantum balance of optical emission and absorption in the system and suggests a stimulated emis-

sion at the frequency ω_2 analogous to stimulated Raman scattering. The multiwave radiation at optical frequencies $\omega_{1,2} \pm l\Omega$ and at microwave cyclotron frequency Ω may provide a method for the observation of cyclo-Raman scattering of any order.

Since the nonparabolicity of the potential well in narrow-gap semiconductors¹² gives rise to a nonlinear mass effect of conduction electron which resembles that of free relativistic electrons, the cyclo-Raman scattering of high orders in such semiconductors may also be expected. Susceptibility $\chi^{(3)}$ for such a process in InSb for $n = 1$ was measured in Ref. 13; hysteretic excitation was predicted in Ref. 14. This process may provide the mechanism for a tunable high-order cyclo-Raman laser in a far-infrared range.¹⁵

In conclusion, we demonstrated the feasibility of the n th-order cyclo-Raman scattering of biharmonic laser by a single cyclotron electron, this effect being characterized by relativistic hysteresises for $n = 1, 2$ and multiple isolas and prohibited orbits for any n .

This work was supported by the U.S. Air Force Office of Scientific Research.

¹A. E. Kaplan, Phys. Rev. Lett. **48**, 138 (1982).

²G. Gabrielse, H. Dehmelt, and W. Kells, Phys. Rev. Lett. **54**, 537 (1985).

³A. E. Kaplan, Nature **317**, 476 (1985); IEEE J. Quantum Electron. **QE-21**, 1544 (1985).

⁴A. E. Kaplan, Phys. Rev. Lett. **56**, 456 (1986).

⁵A. E. Kaplan, Opt. Lett. **12**, 491 (1987).

⁶Y. J. Ding and A. E. Kaplan, Opt. Lett. **12**, 699 (1987).

⁷L. D. Landau and E. M. Lifshitz, *The Classical Theory of Fields* (Addison-Wesley, Cambridge, MA, 1951).

⁸J. L. Hall, C. Salamon, and D. Hils, J. Opt. Soc. Am. B **3**, 80 (1986); P. E. Toschek and J. L. Hall, *ibid.* B **4**, 124 (1987); D. Hils and J. L. Hall, *ibid.* B **4**, 124 (1987).

⁹R. W. P. Drever, J. L. Hall, F. V. Kowalski, J. Hough, G. M. Ford, A. J. Munley, and H. Ward, J. Appl. Phys. B **31**, 97 (1983); K. L. Soohoo, C. Freed, J. E. Thomas, and H. A. Haus, IEEE J. Quantum. Electron. **QE-21**, 1159 (1985); R. G.

DeVoe, C. Fabre, K. Jungmann, K. L. Foster, and R. G. Brewer, J. Opt. Soc. Am. B **3**, 80 (1986).

¹⁰A. E. Kaplan, Radio Eng. Electron. Phys. **8**, 1340 (1963); **9**, 1424 (1964); **11**, 1214 (1966); **11**, 1354 (1966); A. E. Kaplan, Yu. A. Kravtsov, and V. A. Rylov, *Parametric Oscillators and Frequency Dividers*, in Russian (Soviet Radio, Moscow, 1966).

¹¹See, for example, M. Kubicek, I. Stuchl, and M. Marek, J. Comput. Phys. **48**, 106 (1982); T. Erneux and E. Reiss, SIAM J. Appl. Math. **43**, 1240 (1983); J. C. Englund and W. C. Schieve, J. Opt. Soc. Am. B **2**, 81 (1985); A. E. Kaplan and C. T. Law, IEEE J. Quantum. Electron. **QE-21**, 1529 (1985).

¹²E. O. Kane, J. Phys. Chem. Solids **1**, 249 (1957).

¹³E. Yablonovitch, N. Bloembergen, and J. J. Wynne, Phys. Rev. B **3**, 2060 (1971); J. J. Wynne, *ibid.* **6**, 534 (1972).

¹⁴A. E. Kaplan and Y. J. Ding, Opt. Lett. **12**, 687 (1987).

¹⁵See, for example, P. A. Wolff, IEEE J. Quantum. Electron. **QE-2**, 659 (1966).